© 2017. Published by The Company of Biologists Ltd | Development (2017) 144, 345-355 doi:10.1242/dev.139238

TECHNIQUES AND RESOURCES

RESEARCH ARTICLE

TAEL: a zebrafish-optimized optogenetic gene expression system with fine spatial and temporal control

Anna Reade[1], Laura B. Motta-Mena[2,*], Kevin H. Gardner[2,3,4], Didier Y. Stainier[1,5], Orion D. Weiner[1,§] and Stephanie Woo[1,‡,§]

ABSTRACT

Here, we describe an optogenetic gene expression system optimized for use in zebrafish. This system overcomes the limitations of current inducible expression systems by enabling robust spatial and temporal regulation of gene expression in living organisms. Because existing optogenetic systems show toxicity in zebrafish, we re-engineered the blue-light-activated EL222 system for minimal toxicity while exhibiting a large range of induction, fine spatial precision and rapid kinetics. We validate several strategies to spatially restrict illumination and thus gene induction with our new TAEL (TA4-EL222) system. As a functional example, we show that TAEL is able to induce ectopic endodermal cells in the presumptive ectoderm via targeted *sox32* induction. We also demonstrate that TAEL can be used to resolve multiple roles of Nodal signaling at different stages of embryonic development. Finally, we show how inducible gene editing can be achieved by combining the TAEL and CRISPR/Cas9 systems. This toolkit should be a broadly useful resource for the fish community.

KEY WORDS: Optogenetics, Zebrafish, Gene expression, Endoderm, Nodal, CRISPR, Cas9

INTRODUCTION

Extensive insight into pathways involved in biological processes and the components that make up these pathways has been achieved through traditional genetic methods. However, biological systems can exhibit compensation over the time scale that is required to create stable transgenic or mutant lines, thereby obscuring gene function. Additionally, when working with multicellular organisms it is often difficult to limit a perturbation to a specific set of cells, and it can be challenging to perturb genes that are expressed at multiple developmental stages or that are essential for survival. Therefore, the ability to precisely control the location, amount and timing of gene expression would be transformative for the cell and developmental biology communities.

In zebrafish, as well as other multicellular model organisms, current inducible gene expression systems are quite limited in their degree of spatial and temporal control. Temporal control has been achieved through the administration of small molecule compounds, such as in the tetracycline-inducible expression system (Knopf et al., 2010), or activation of heat shock promoters (Shoji and Sato-Maeda, 2008). In the case of small molecule-dependent activation, timing and penetration can be variable and difficult to control. The use of the heat shock promoter improves upon these issues but introduces the confounding factor of inducing a stress response in the organism as well. For either of these inducible systems, spatial control is mostly achieved by use of tissue-specific promoters (Hesselson et al., 2009), but this approach is limited by the existence of a reliable tissue-specific promoter and is not capable of sub-tissue level control.

One promising technique for finer spatial and temporal control of gene expression is to use optogenetic transcriptional activators for light-based control of transcription (Tischer and Weiner, 2014). Several optogenetic gene expression systems have been developed (Shimizu-Sato et al., 2002; Yazawa et al., 2009; Kennedy et al., 2010; Ye et al., 2011; Ohlendorf et al., 2012; Polstein and Gersbach, 2012, 2015; Liu et al., 2012; Wang et al., 2012; Chen et al., 2013; Motta-Mena et al., 2014), but so far, these systems are non-optimal for use in zebrafish. An ideal zebrafish optogenetic system would be genetically encoded, not require complicated optics or exogenous small molecules, have a large range of induction, be reversible with fairly rapid kinetics and, importantly, have little to no toxicity.

Two recently reported light-gated transcriptional systems, LightOn (Wang et al., 2012; Chen et al., 2013) and EL222 (Motta-Mena et al., 2014), are promising candidates for spatiotemporal control of transcription in zebrafish. Both systems make use of an engineered light-oxygen-voltage (LOV) protein that dimerizes when illuminated with blue light (Crosson et al., 2003; Zoltowski et al., 2013; Fig. 1A). The LightOn system is based on a synthetically constructed transcriptional activator, GAVPO, consisting of the LOV domain from the *Neurospora* protein Vivid fused to both a Gal4 DNA-binding domain and a p65 transactivating domain. Upon light-induced dimerization, GAVPO binds to its corresponding UAS promoter and induces transcription of a gene of interest (Wang et al., 2012; Chen et al., 2013). The EL222 system relies on similar principles but is based on a naturally occurring light-responsive transcription factor, EL222, found in *Erythrobacter litoralis*. EL222 contains a LOV domain followed by a helix-turn-helix (HTH) DNA-binding domain, which binds to a regulatory element termed C120 (Nash et al., 2011; Rivera-Cancel et al., 2012). Adding a VP16 transactivating domain and nuclear localization signal to EL222 created the engineered transcriptional activator VP-EL222 (Motta-Mena et al., 2014).

Here, we have tested the LightOn and EL222 optogenetic transcriptional systems in zebrafish and found that while both are easily expressed and capable of inducing strong gene expression in a light-gated manner, they produced various degrees of toxicity in the

[1]CVRI & Department of Biochemistry and Biophysics, University of California, San Francisco, San Francisco, CA 94158, USA. [2]Structural Biology Initiative, CUNY Advanced Science Research Center, City University of New York, New York, NY 10031, USA. [3]Department of Chemistry and Biochemistry, City College of New York, New York, NY 10031, USA. [4]Biochemistry, Chemistry and Biology PhD Programs, Graduate Center, The City University of New York, New York, NY 10016, USA. [5]Max Planck Institute for Heart and Lung Research, Dept. of Developmental Genetics, Bad Nauheim 61231, Germany.
*Present address: Optologix, Inc., 1910 Pacific Ave., Suit 20000, Dallas, TX 75201, USA. ‡Present address: School of Natural Sciences, University of California-Merced, Merced, CA 95343, USA.

§Authors for correspondence (orion.weiner@ucsf.edu; swoo6@ucmerced.edu)

S.W., 0000-0002-1238-8167

Received 28 April 2016; Accepted 28 November 2016

Development (2017) 144, 345-355 doi:10.1242/dev.139238

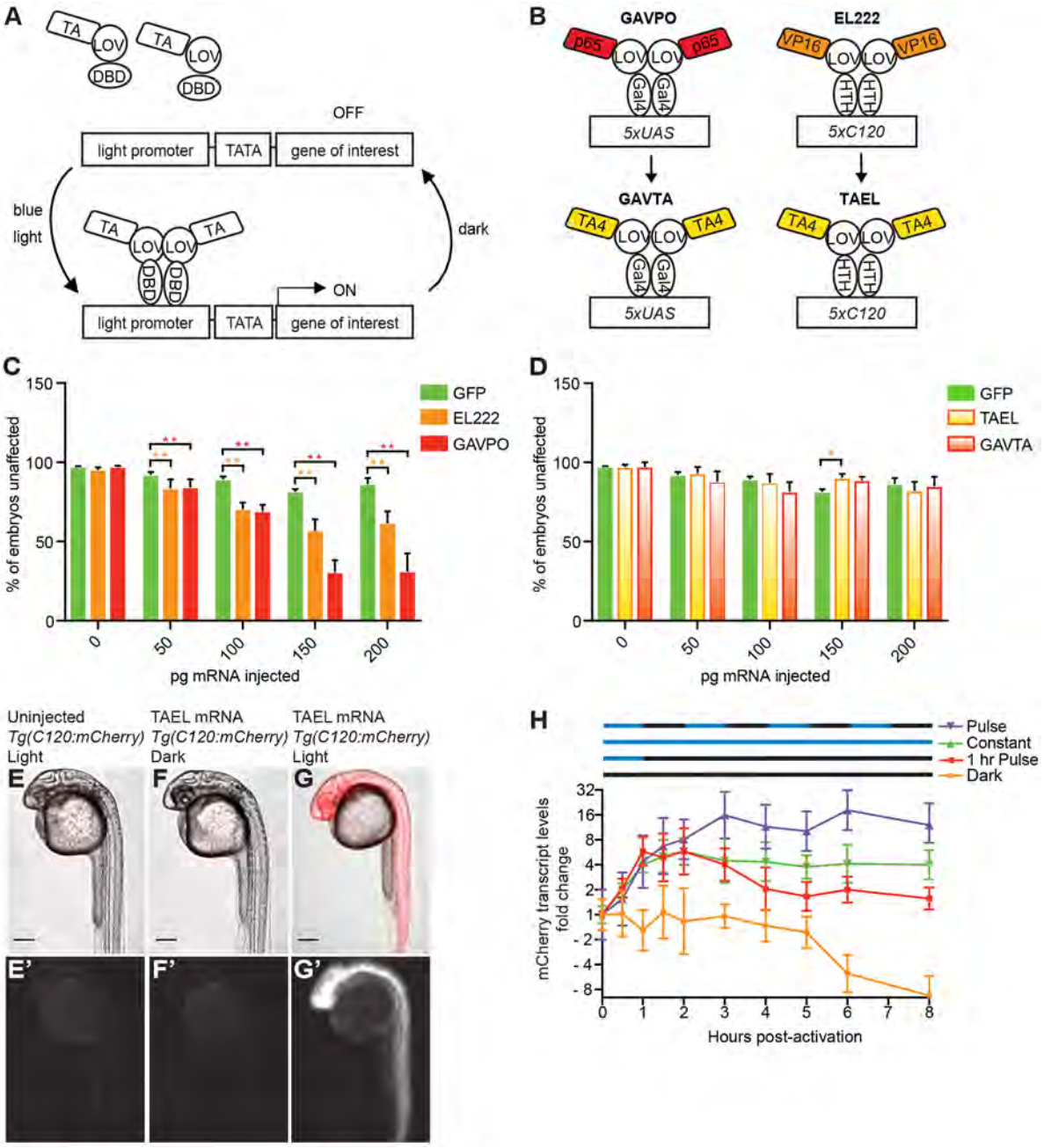

Fig. 1. Optimization of TAEL as an optogenetic gene expression system for zebrafish. (A) Schematic depicting general mechanism for single-protein component, LOV-based, light-responsive gene expression systems. (B) Schematic depicting transcriptional activators. (C,D) Percentage of unaffected, healthy embryos per amount of mRNA injected. Injection of GAVPO or EL222 mRNA is significantly more toxic compared with the equivalent amount of GFP control mRNA (C), but GAVTA and TAEL mRNA injections produce less toxicity (D). **P*<0.05, ***P*<0.0001, two-tailed Fisher's exact test. GFP data in D reproduced from C. Data represent mean percentage (±s.e.m.) of total embryos (*n*) from 2-3 independent experiments. GAVPO, *n*=849 embryos; EL222, *n*=1421 embryos; GFP, *n*=1190 embryos; GAVTA, *n*=809 embryos; TAEL, *n*=824 embryos. (E-G) TAEL induces robust mCherry transcription from the *C120* promoter at 24 hpf (G,G′), with no visible induction of mCherry expression in dark (F,F′) or uninjected controls (E,E′). Scale bars: 200 µm. (H) qPCR analysis of TAEL-induced *mCherry* expression over time, normalized to 0 h post-activation for each illumination pattern. Pulsed illumination (purple line) results in stronger induction compared with constant illumination (green line). Red dotted line shows that *mCherry* transcription quickly turns off after activated embryos are returned to dark conditions. Embryos kept in the dark for all time points exhibit baseline *mCherry* expression (orange line). Data represent means±s.e.m. from three biological replicates, each with three technical replicates. *Y*-axis is displayed on a $\log_2$ scale.

embryos. We then re-engineered each system to be less toxic, but only the modified EL222 system, which we have named TAEL (for TA4-EL222), maintained functionality in zebrafish embryos. We go on to show that TAEL exhibits a large range of induction with relatively rapid on/off kinetics, and we use several different methods to spatially pattern blue light delivery to activate the TAEL system in a spatially restricted manner. Finally, we demonstrate the functionality of the TAEL system by generating ectopic endodermal cells via s*ox32* induction, modulating the temporal dynamics of Nodal signaling by inducing *lefty1* expression, and inducing CRISPR-directed gene mutations through TAEL-dependent expression of Cas9 nuclease.

Development (2017) 144, 345-355 doi:10.1242/dev.139238

RESULTS

Optimization and characterization of TAEL, an optogenetic gene expression system for zebrafish

Two LOV-based optogenetic expression systems, LightOn and EL222, were recently developed (Wang et al., 2012; Chen et al., 2013; Motta-Mena et al., 2014). We previously showed that the EL222 system could function in zebrafish embryos (Motta-Mena et al., 2014). Therefore, we first sought to test whether the LightOn system functioned similarly in zebrafish. We injected GAVPO mRNA into single-cell stage *Tg(UAS:kaede)* embryos, then exposed embryos to constant, global blue light (465 nm) from ∼4 to 24 hours post-fertilization (hpf). GAVPO-injected embryos showed robust induction of Kaede fluorescent protein at 24 hpf with no visible induction of Kaede expression in dark or uninjected controls (Fig. S1A-C).

To compare the relative toxicity of VP-EL222 and GAVPO, we performed a toxicity curve for each transcriptional activator. Embryos were injected with increasing amounts of VP-EL222 or GAVPO mRNA then scored as unaffected or affected (deformed or dead) at 1 day post-fertilization (dpf). At each concentration tested, both transcriptional activators were more toxic to zebrafish development than a GFP control mRNA (Fig. 1C).

High levels of strong transactivating domains have previously been shown to be toxic during zebrafish development (Distel et al., 2009). To ameliorate their toxicity, we replaced the VP16 or p65 domain of VP-EL222 and GAVPO, respectively, with the transactivating domain of KalTA4, which has been reported to be better tolerated in zebrafish embryos (Baron et al., 1997; Distel et al., 2009) (Fig. 1B). Toxicity curves were repeated for both modified transcriptional activators, TA4-EL222 and GAVPO-TA4 (shortened to TAEL and GAVTA, respectively). Injection of both TAEL and GAVTA produced little to no toxicity even up to 200 pg of injected mRNA/embryo (Fig. 1D). We then determined whether the modified constructs retained their light-based transcriptional activation function. Injection of GAVTA mRNA into *Tg(UAS:kaede)* embryos and subsequent exposure to blue light was no longer able to induce Kaede expression (Fig. S1D-F) compared with the original GAVPO construct (Fig. S1A-C). However, TAEL mRNA injection into *Tg(cryaa:Venus;C120:mcherry)* embryos still induced strong mCherry expression under blue light conditions with a slight developmental delay (Fig. 1G,G′). No visible mCherry expression was observed in embryos kept in the dark (Fig. 1F,F′). As a result, only the TAEL system was pursued for subsequent experiments.

Previously, the original VP-EL222 construct was shown to have rapid activation (<10 s) and deactivation kinetics (<50 s) in cultured human cells (Motta-Mena et al., 2014). To evaluate the kinetics and range of the modified TAEL construct, we performed a time course analysis of TAEL-induced gene expression. *Tg(cryaa:Venus;C120:mcherry)* embryos were injected with 100 pg TAEL mRNA and exposed to global blue light starting at 3.5 hpf. mCherry transcript levels were measured by qPCR at various time points post-illumination (Fig. 1H). Because the original VP-EL222 construct was found to respond optimally to pulsed illumination, we compared TAEL-induced mCherry expression under both constant and pulsed (1 h on, 1 h off) illumination. At 1 hour post-activation (hpa), both regimes resulted in significant upregulation of mCherry expression relative to initial (0 hpa) levels (Fig. S3). However, we observed that over time, pulsed illumination resulted in stronger mCherry induction compared with constant illumination (two-way ANOVA, $F_{1,40}$=6.803, P=0.0127). Under pulsing blue light, mCherry expression reached a peak of approximately 16-fold upregulation at 3 hpa that was sustained up to 8 hpa, whereas with constant illumination, maximum mCherry induction was around 6-fold (Fig. 1H). This difference is likely to be due to photodamage of the LOV domain of the TAEL transcriptional activator under chronic blue light illumination.

To examine the deactivation kinetics of the TAEL system, we exposed embryos to 1 h of activating blue light, which is sufficient to induce a significant increase in mCherry expression (Fig. S3), and then returned them to the dark and measured mCherry expression at several time points thereafter. We observed no new mCherry transcription within 30 min following removal from blue light illumination (Fig. 1H), showing TAEL deactivation kinetics to be relatively rapid.

We also used qPCR analysis to assess the leakiness of the TAEL system. First, we determined whether there was spurious activation of the LOV domains of TAEL by measuring mCherry mRNA expression levels in *Tg(cryaa:Venus;C120:mcherry)* embryos injected with *TAEL* mRNA but kept in the dark. We found that although mCherry transcripts could be detected, expression was at much lower levels than in illuminated embryos (Fig. 1H). We also measured mCherry mRNA levels from uninjected *Tg(cryaa:Venus;C120:mcherry)* embryos to assess the leakiness of the *C120* promoter itself, which was previously reported to have some basal activity in cultured human cells (Motta-Mena et al., 2014). We did observe some basal mCherry expression, but at much lower levels than in illuminated, TAEL-injected embryos (Fig. S2).

Spatial control of TAEL induction

A major advantage of the TAEL system over previous gene expression systems is its ability to control its activation spatially by controlling the illumination pattern of activating blue light. Since the range of blue light that can activate TAEL's LOV domain is from 450-490 nm (Motta-Mena et al., 2014; Nash et al., 2011), the GFP channel's excitation light on any microscope can be used as an activating light source. We tested four different methods for delivering spatially restricted blue light: (1) Closing down the field diaphragm on an epifluorescence microscope, which restricts light to a small hexagonal column (Fig. 2A,B); (2) defining a region of interest (ROI) on a point scanning confocal microscope to restrict scanning to a small square (Fig. 2C,D); (3) using a digital micromirror device (DMD) (Sakai et al., 2013) illuminated with a 470 nm LED to project various-sized square columns of blue light onto our samples (Fig. 2E-H); and (4) restricting the scanning range on a digital scanned laser light sheet microscope (DSLM) (Maizel et al., 2011) to deliver beams of blue light of varying widths (Fig. 2I-L). For each method, *Tg(cryaa:Venus;C120:mcherry)* embryos were injected with TAEL mRNA and the eye region was illuminated with a single 2 min pulse of blue light at the 10-somite stage. mCherry fluorescence was then assessed ∼4 h later.

Each of the tested methods succeeded in activating expression of mCherry in the eye region. Qualitatively, we observed that illumination and expression patterns were mostly correlated such that more restricted applications of blue light resulted in more restricted regions of mCherry expression (e.g. compare Fig. 2E-F′ to Fig. 2G-H′). However, we did sometimes observe mCherry fluorescence in areas outside the eye (brackets, Fig. 2L,L′). This apparent 'off-target' expression is most likely due to scattering of activating blue light through the thick tissue of the head but may also arise from cells migrating out of the target region between the time periods of activation and assessment of mCherry fluorescence.

Of the four methods tested, mCherry induction with the point scanning confocal was the least successful, which could be due to either the instantaneous intensity of the point scanner being too high (essentially photo-bleaching the TAEL protein), or the local dwell

Development (2017) 144, 345-355 doi:10.1242/dev.139238

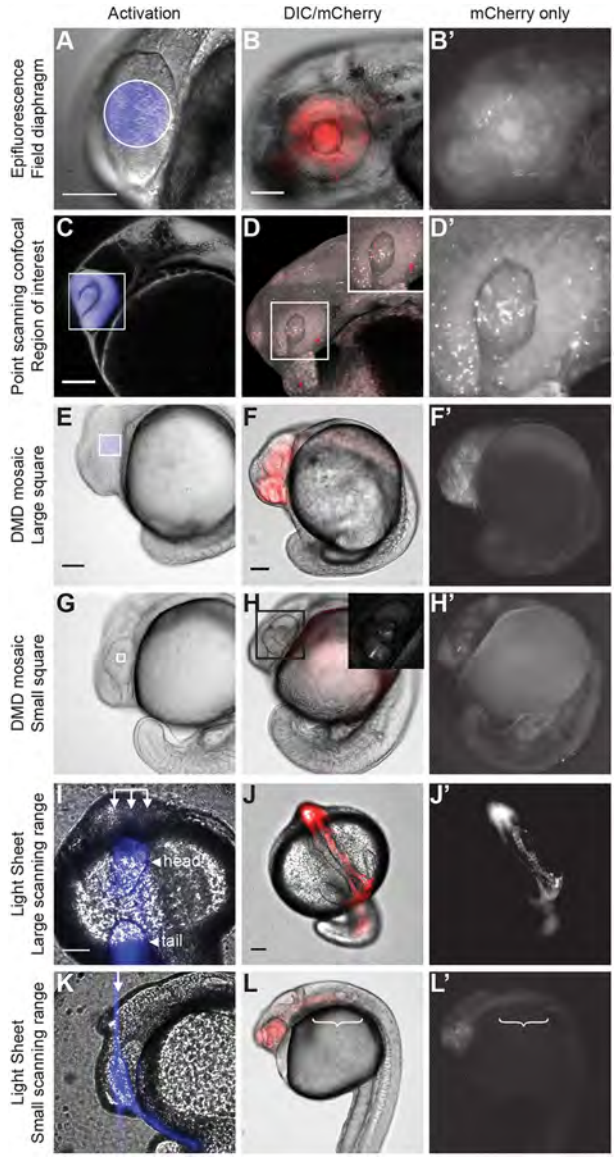

Fig. 2. Spatial control of TAEL induction achieved using four different imaging modalities. Left column shows activation region (blue) for each method. Middle and right columns show resulting mCherry expression (red) 4 h post-activation. (A,C,E,G,I,K) Bright-field and 488 nm channels merged. (B,D,F,H,J,L) Bright-field and 561 nm channels merged. (B′,D′,F′,H′,J′,L′) 561 nm channel only. Unless otherwise noted, images are lateral views with rostral to the left. (A-B′) Closing down the field diaphragm on an epifluorescence microscope (488 nm, GFP excitation setting) restricts the light coming through the objective and illuminates the sample with a small hexagonal column. (C-D′) Region of interest (ROI) on a point scanning confocal to restrict scanning of the 488 nm laser to a small square. (E-H′) Digital micromirror device (DMD) illuminated with a 470 nm LED to project variously sized square columns of blue light onto the embryo. (I-L′) Restricted scanning range of the 488 nm laser on a digital scanned laser light sheet microscope (DSLM) to project variously wide beams of blue light through the embryo. (I) *En face* view with head and tail as indicated. (J-J′) Dorsal view with anterior to the bottom. Brackets (L,L′) indicate an example of 'off-target' mCherry expression. Arrows in I and K indicate position of the light sheet. Scale bars: 100 µm.

time of the beam being too short for TAEL activation (the scan speed of 400 Hz is the slowest possible on the Leica SPE). In contrast, we found that epifluorescence with a restricted field diaphragm most consistently induced strong mCherry expression. In fact, we found that this method delivered the strongest intensity of light, suggesting that light intensity is a crucial consideration (epifluorescence, 1800 mW/cm^2; DMD, 1.7 mW/cm^2; point scanner, 16.6 µW scanned at 400 Hz over 175 µm^2 region; DSLM, 100 µW scanned over 133 or 20 µm).

Ectopic endoderm induction via light-induced expression of Sox32

As a functional test of using the TAEL system to achieve spatially restricted gene expression, we sought to produce ectopic endoderm by inducing expression of the transcription factor Sox32 in the presumptive ectoderm of early stage embryos (Fig. 3). Sox32 is known to be both necessary and sufficient for endoderm fate specification (Kikuchi et al., 2001; Alexander et al., 1999; Pézeron et al., 2008). We first created a stable transgenic line with *sox32* under the control of the *C120* promoter [*Tg(cryaa:Venus;C120:sox32)*] and then crossed this line to *Tg(sox17:GFP)* transgenic fish to label endodermal cells (Fig. 3A). We then injected TAEL mRNA along with a nuclear marker, H2B-mCherry mRNA, into *Tg(cryaa:Venus;C120:sox32);Tg(sox17:GFP)* embryos. At 3-4 hpf, we used a narrowed field diaphragm on an epifluorescence microscope to restrict activating illumination to the animal pole (Fig. 3B, top panel), targeting presumptive ectoderm and part of the enveloping layer (EVL) (Kimmel et al., 1990). We then assessed ectopic endoderm production at 6-7 hpf using *Tg(sox17:GFP)* as a marker for endodermal fate. At this stage, the embryo has undergone gastrulation so that endodermal cells lie in the innermost layer closest to the yolk (Fig. 3B, bottom panel) while ectodermal and EVL cells reside in the outer layers. Embryos that lacked TAEL mRNA exhibited wild-type endoderm distribution (Fig. 3L and Movie 1) as did embryos injected with TAEL but kept in the dark (Fig. 3M and Movie 2), with GFP-positive cells restricted to a single inner layer. However, within activated embryos, GFP-positive cells were found in multiple layers with a number of GFP-positive cells in the outer EVL and ectodermal layers (Fig. 3E,N and Movie 3).

Temporal control of TAEL induction: dissecting multiple roles of Nodal signaling during embryonic development

As our qPCR data indicated that TAEL exhibits relatively fast activation kinetics (Fig. 1G), we next sought to apply the TAEL system to temporally control gene expression. To demonstrate such temporal control, we used the TAEL system to interrogate the Nodal signaling pathway at different stages of zebrafish development. Nodal has a very well defined role in specifying mesendoderm early in development (Feldman et al., 1998; Peyriéras et al., 1998; Gritsman et al., 1999; Thisse and Thisse, 1999; Thisse et al., 2000). However, Nodal also acts at later stages to pattern the left-right axis of the embryo (Rebagliati et al., 1998; Yan et al., 1999; Essner et al., 2000). Traditional loss-of-function techniques such as genetic mutations or morpholino knockdown are not able to distinguish between these two functions. Therefore, we used the TAEL system to induce expression of the secreted Nodal antagonist *lefty1* either during early development to block mesendoderm specification or during somitogenesis stages to interfere with left-right patterning independent of mesendoderm formation (Fig. 4). We constructed a transgene containing *lefty1* under control of the *C120* promoter (Tol2-5xC120:lefty1) and injected this plasmid into embryos along with TAEL mRNA. Injected embryos were then illuminated globally with 465 nm blue light from 2 to 8 hpf (early) or from 12 to 24 hpf (late) (Fig. 4A). We found that when embryos were activated early they exhibited a range of phenotypes indicative of loss of meso- and endodermal tissues, including a shortened embryonic axis (Thisse et al., 2000) (Fig. 4D) and cyclopia (Thisse

Development (2017) 144, 345-355 doi:10.1242/dev.139238

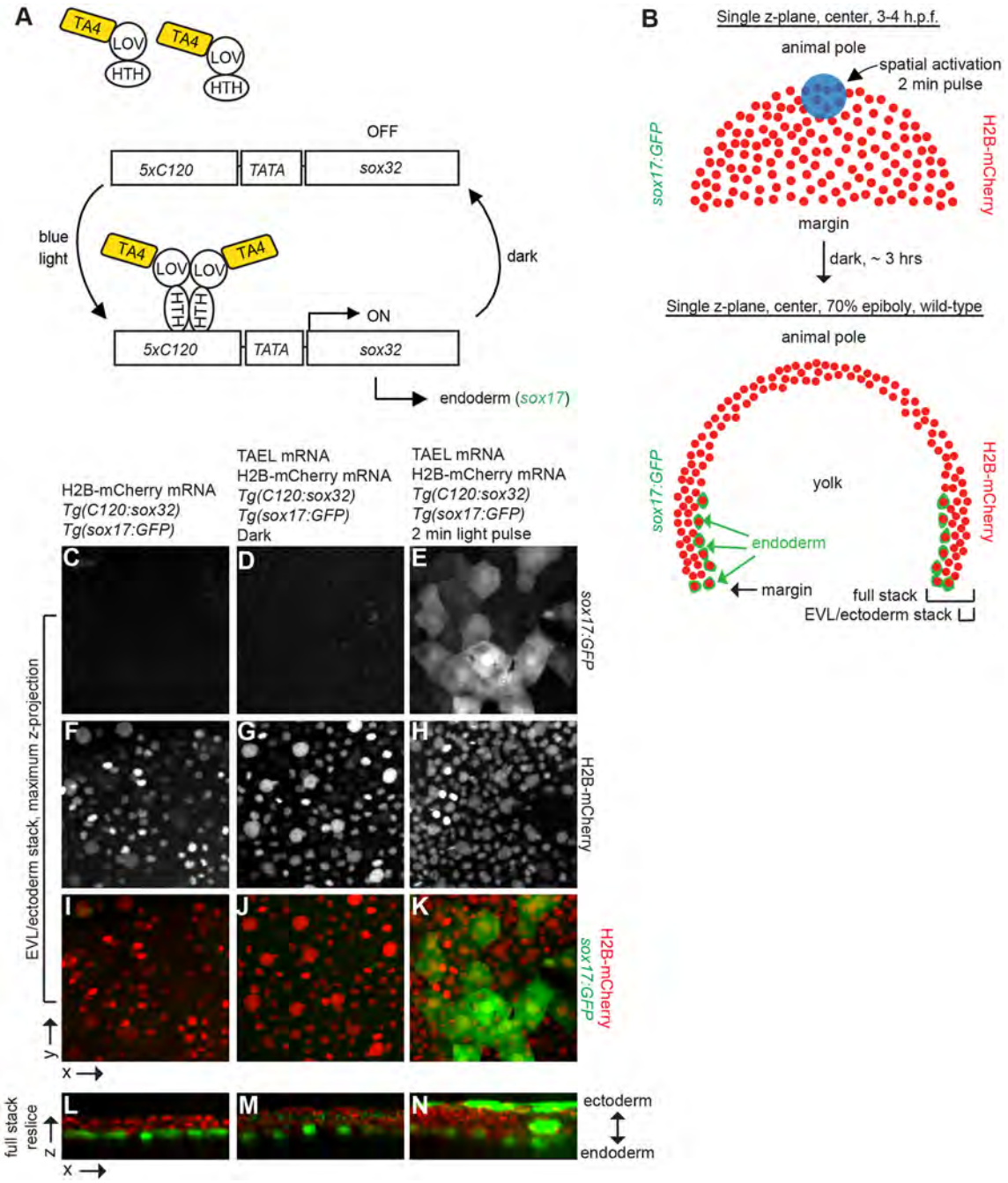

Fig. 3. Conversion of presumptive EVL and ectoderm to endoderm via TAEL-dependent Sox32 expression. (A) Schematic depicting experimental set-up for light-induced endoderm induction. *Tg(cryaa:Venus;C120:sox32); Tg(sox17:GFP)* embryos were injected with TAEL mRNA. Ectoderm progenitors at the animal pole were illuminated with blue light, leading to misexpression of *sox32* and adoption of endoderm fate (expression of sox17:GFP). (B) Top panel depicts an embryo at 3-4 hpf with nuclei labeled by H2B-mCherry (red). Activating light was restricted to the animal pole (blue circle, approximately 116 µm in diameter). Bottom panel depicts a transverse cross section of an embryo at 70-80% epiboly. Endodermal cells are labeled by *Tg(sox17*:GFP*)* (green) and all nuclei are labeled with H2B-mCherry (red). Brackets labeled 'EVL/ectoderm stack' and 'Full stack' indicate approximate positions of images shown in C-K and L-N, respectively. (C-K) Maximum *z*-projections of EVL and ectoderm layers only. Embryos lacking TAEL (C) or expressing TAEL but kept in the dark (D) show no GFP-positive cells in these layers. However, activated embryos (E) exhibit numerous GFP-positive cells within the EVL and ectoderm domain. (L-N) Re-sliced *x-z* views of the entire acquired stack (EVL/ectoderm towards the top, endoderm toward the bottom). In embryos lacking TAEL (L) or expressing TAEL but kept in the dark (M) GFP-positive cells are restricted to a single endodermal layer adjacent to the yolk, whereas in activated embryos (N), GFP-positive cells are located in multiple cell layers, especially in the outer EVL and ectoderm domains. Uninjected, 17% with ectopic endoderm, *n*=17; dark, 33% with ectopic endoderm, *n*=9; light activated, 65% with ectopic endoderm, *n*=17.

and Thisse, 1999) (Fig. 4H). These defects were not seen in late-activated embryos (Fig. 4E,I), suggesting that mesendoderm patterning was not affected. To determine effects on left-right patterning, we assessed heart looping at 48 hpf. In uninjected embryos (Fig. 4J) or injected embryos kept in the dark (Fig. 4K), most hearts exhibited normal asymmetric looping (uninjected, 90.9% looped, *n*=55; dark, 70% looped, *n*=10). However, the majority of late-activated embryos exhibited no heart looping

Development (2017) 144, 345-355 doi:10.1242/dev.139238

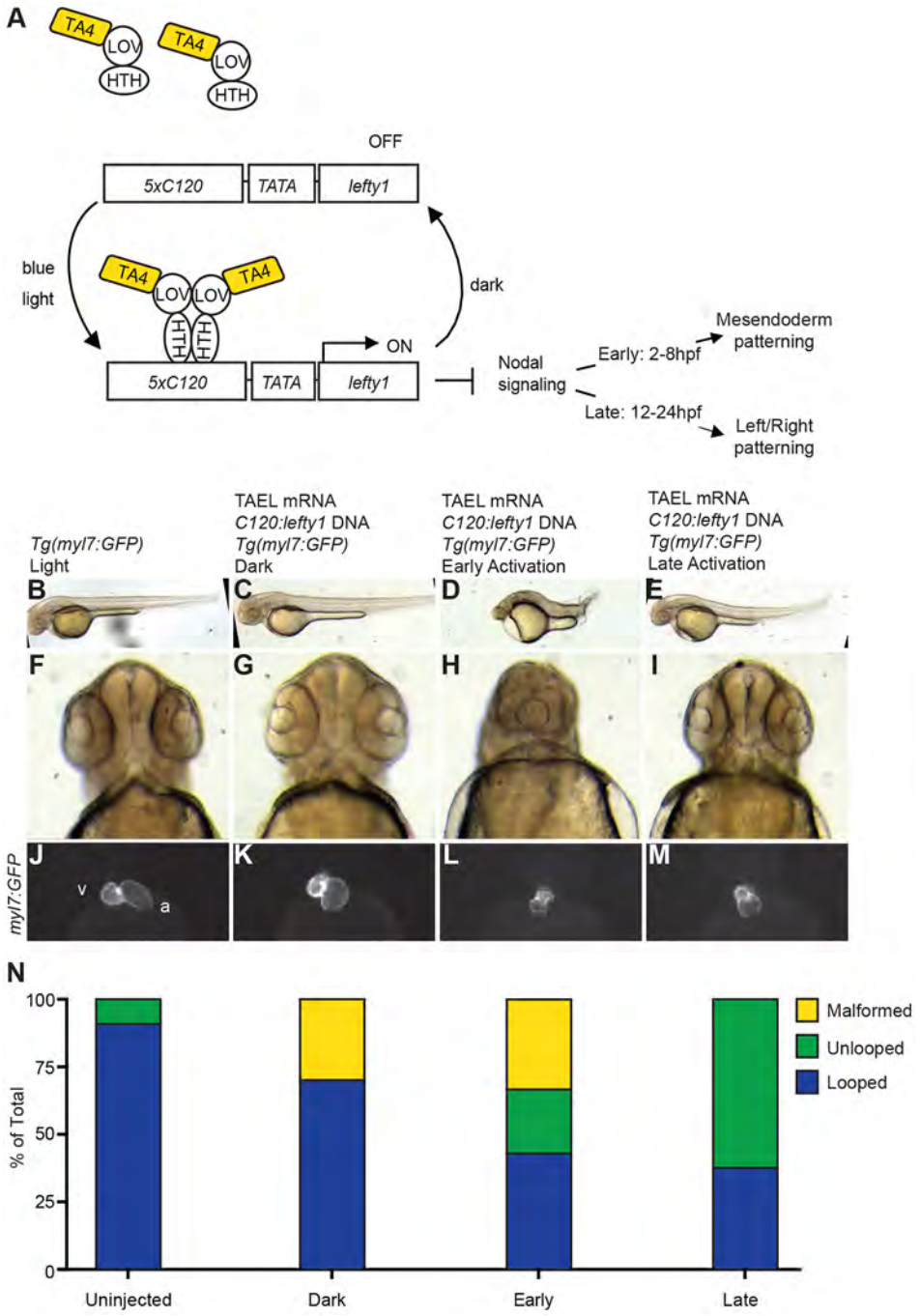

Fig. 4. Temporal control of Nodal signaling via TAEL-induced expression of *lefty1*. (A) Schematic depicting experimental set-up for TAEL-induced Nodal inhibition. Embryos were injected with a transgene containing the *C120* promoter driving expression of the Nodal antagonist *lefty1* along with TAEL mRNA. Embryos were then globally illuminated with blue light either from 2-8 hpf (early) or 12-24 hpf (late). (B-E) Lateral views of embryos at 48 hpf show that early activation results in severely shortened embryonic axis (D) whereas late activation does not affect body length (E). (F-I) Rostral views of 48 hpf embryos show that early (H) but not late (I) activation produces cyclopia, indicative of loss of cephalic mesoderm. (J-M) Ventral views of 48 hpf embryos with hearts labeled by *Tg(myl7*:GFP*)* expression. Control embryos exhibit asymmetric heart looping (J,K). In contrast, late activation of *lefty1* expression produces unlooped hearts with both chambers located at the midline (M). Early activation produced both unlooped and malformed hearts (L). A, atrium; V, ventricle. (N) Quantification of heart defects. Uninjected, *n*=55; dark, *n*=10; early, *n*=21; late, *n*=24.

(62.5% unlooped, *n*=24). Instead, both cardiac chambers were located at the midline, suggesting a lack of left-right asymmetry (Fig. 4L). Unlooped hearts were also observed to a lesser extent in early-activated embryos (23.8%, *n*=21), although under this condition many hearts were too malformed to accurately assess looping. Together, these experiments demonstrate that the TAEL system enables temporal control of gene expression and can be used to study signaling pathways at multiple stages of development.

Spatiotemporal control of the CRISPR system

One potentially powerful use of the TAEL system involves controlling the expression of Cas9 to achieve targeted, spatiotemporally controlled gene editing. The RNA-guided nuclease Cas9 is a key component of clustered, regularly interspaced, short palindromic repeat (CRISPR) technology, which has become a widespread, powerful tool for rapid and efficient genome editing (Sander and Joung, 2014). A light-gated split Cas9/CRISPR system was recently developed (Nihongaki et al., 2015). However, like other optogenetic gene expressions systems developed before TAEL, it has not been optimized for use in zebrafish nor shown to function in multicellular organisms in general. Additionally, the TAEL system would provide a more general platform for controlling Cas9 expression, which could be combined with the light-gated expression of other genes of interest. To test the feasibility of light-gated genome editing, we built a three promoter transgene construct containing: (1) the heart-specific promoter *myl7* driving GFP expression as a transgenesis marker;

Development (2017) 144, 345-355 doi:10.1242/dev.139238

(2) Cas9 under the control of the *C120* promoter; and (3) a *U6* promoter (Ablain et al., 2015) driving ubiquitous expression of a guide RNA sequence targeting *tyrosinase* (*tyr*), a gene essential for proper pigment formation (Haffter et al., 1996) (Fig. 5A). TAEL mRNA was co-injected with this construct into wild-type embryos, which were then illuminated globally with 465 nm blue light from 3 to 8 hpf. Pigmentation was assessed at 2 dpf. Notably, ∼90% of illuminated embryos (n=18) showed various levels of pigment disruption (Fig. 5D), demonstrating light-induced editing of the *tyr* gene using TAEL. In contrast, 100% of dark control embryos examined (n=11; Fig. 5C) exhibited pigmentation comparable to wild-type uninjected embryos (Fig. 5B). We also assayed TAEL-induced genome editing by CEL I nuclease digestion of the targeted *tyr* locus (Fig. 5E) (Till et al., 2004). We observed smaller cleavage fragments, which are indicative of mutagenesis, in illuminated embryos but not in non-illuminated or uninjected control embryos.

DISCUSSION

Our TAEL optogenetic transcriptional control system offers several advantages over current inducible gene expression systems in zebrafish. First, this system does not require an exogenous component in order to function because the flavin chromophore that the LOV domain requires to respond to light is endogenous to zebrafish (Motta-Mena et al., 2014; Crosson et al., 2003; Nash et al., 2011). This is not the case in phytochrome-based optogenetics, which requires the addition of phycocyanobilin in order to function (Tischer and Weiner, 2014; Shimizu-Sato et al., 2002; Buckley et al., 2016). Additionally, TAEL is genetically encoded and composed of a single homodimerizing transcriptional activator. This single component aspect eliminates the need for expression optimization of multiple proteins as with the Cry2/Cib system (Liu et al., 2012).

We also demonstrate that the TAEL system has a large dynamic range and relatively rapid on and off kinetics within the time scale of

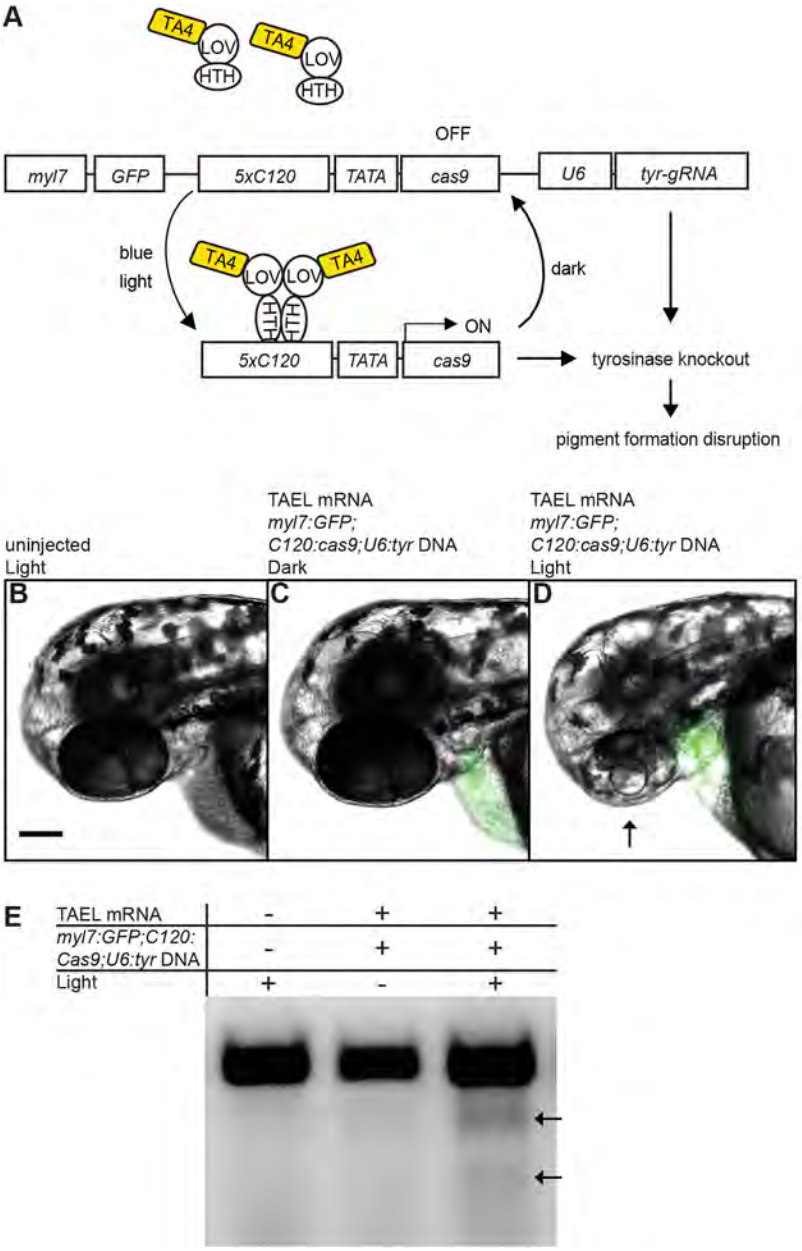

Fig. 5. Light-induced gene editing in zebrafish. Light-induced gene knockout can be achieved by combining the TAEL system with the CRISPR/Cas9 system. (A) Three promoter construct containing: (1) the heart-specific promoter *myl7* in front of GFP to label injected embryos, (2) Cas9 under the control of the *C120* promoter and (3) a *U6* promoter in front of the guide RNA sequence targeting tyrosinase, a protein essential for pigment formation. TAEL mRNA was co-injected with the construct depicted in A into wild-type single-celled embryos. Embryos were illuminated globally with 465 nm blue light and then scored for disruption in pigment formation at 2 dpf. (B-D) Wild-type, uninjected embryos (B) exhibit normal pigmentation as do injected dark controls (C). Pigment formation is disrupted in injected and illuminated embryos (D, arrow). Approximately 90% of illuminated embryos (n=18) showed various levels of pigment disruption, while 100% of dark control embryos examined (n=11) exhibited pigmentation comparable to wild-type uninjected embryos. (E) Representative CEL I nuclease assay indicates mutagenesis of the *tyr* locus in illuminated but not dark or uninjected control embryos. Arrows indicate cleavage fragments. Scale bar: 100 µm.

Development (2017) 144, 345-355 doi:10.1242/dev.139238

gene expression. Our results suggest that by varying the amount of blue light illumination, various transcriptional outputs can be generated. For example, we found that constant blue light illumination induced lower expression compared with illumination pulsed at 1 h intervals; perhaps other pulsing frequencies can be used to further increase gene expression levels. Lower levels of transient transcription can be achieved with single blue light pulses of as little as 2 min. However, our results also indicate that chronic or extremely high intensity blue light exposure appears to photodamage the LOV domain of the TAEL activator (data not shown), which should be taken into consideration when using the TAEL and other LOV-based systems. Finally, we showed that once returned to a dark state, the TAEL system stops all new transcription within 30 min. These data suggest that varying the strength and timing of blue light activation should enable user-defined levels of gene induction. Induction levels could also be tuned by making minor modifications to TAEL system components. For example, combination with the Gal4/UAS system could be used to amplify expression levels (Halpern et al., 2008). Changing the basal promoter attached to the *C120* regulatory element, which currently uses a minimal TATA box, could also attenuate or amplify expression. Many different basal promoters have been used in zebrafish transgenesis and the choice of basal promoter can affect transcriptional output (Scott and Baier, 2009).

Of note, we did sometimes observe developmental delay upon TAEL activation (for example, Fig. 5). However, the embryos always recovered and no other abnormalities were observed. Similar developmental delays occur with the heat shock promoter (*hsp70*) system (data not shown). Therefore, developmental delay may be a common consequence of inducible expression systems caused by an acute and/or overwhelming mobilization of the transcriptional machinery.

The greatest advantage of the TAEL system is its high level of spatial control. Here, we demonstrate that complicated optics are not required to activate the TAEL system in a spatially restricted manner (Fig. 2). Spatial restriction of induction can be as simple as closing down the field diaphragm on an epifluorescence microscope and illuminating the sample for as little as 2 min. Indeed, we demonstrated that this technique was sufficient to drive presumptive ectoderm to express endodermal markers through targeted induction of *sox32* (Fig. 3). Higher levels of control can also be achieved by using more advanced methods of blue light application. For example, using the ROI function on a point scanning confocal microscope can restrict the 488 nm channel to a specific area of interest, as can a DMD fitted with an LED in the 450-490 nm range. For light sheet microscopes, restricting the sheet height or the area in which the laser is scanned is another means to spatially control activation.

Our qPCR data suggested that TAEL-dependent transcription exhibits rapid on-off kinetics (Fig. 1H), allowing for precise temporal control of gene expression. Most signaling pathways are employed at multiple stages of embryonic development, and it can be challenging to distinguish among these different roles using traditional loss-of-function techniques. Here, we used the TAEL system to examine the role of Nodal signaling in both mesendoderm specification and left-right patterning (Fig. 4), demonstrating that our system can be a useful tool for interrogating the roles of widely expressed signaling molecules during specific developmental processes. Its rapid kinetics will also enable use of the TAEL system in situations with crucial temporal dynamics, such as for testing competency windows.

With the versatility that we have demonstrated, the TAEL system could serve a multitude of different functions. It can be used to express genes of interest at any time and location, which is extremely useful for studying a gene or pathway that is expressed at multiple locations or times during development. Furthermore, the TAEL system can be used for spatiotemporal control of gene editing via induction of *Cas9*. This TAEL/CRISPR combination could be used to improve our ability to study traditionally difficult to perturb genes, such as those essential for survival or those that function in multiple tissues and/or developmental stages. It could also be used to test the cell autonomy of gene function by inactivating the gene of interest in a subset of cells while leaving the surrounding tissue unaffected. This zebrafish-optimized light-gated gene expression system should be a broadly useful resource for the fish community.

MATERIALS AND METHODS

Vector construction and mRNA synthesis

Expression plasmid pCS2-(VP16)EL222 has been described previously (Motta-Mena et al., 2014). All sub-cloning was done by Gibson assembly (Gibson et al., 2009). Expression plasmid pCS2-GAVPO was created by PCR amplification of GAVPO ORF (Wang et al., 2012) and then cloned into pCS2+. Expression plasmid pCS2-TAEL was created by PCR amplification of TA4 ORF of KalTA4 (Distel et al., 2009) and then cloned into pCS2-(VP16)EL222 cut with *Eco*RI and *Nco*I to remove the VP16 domain. Expression plasmid pCS2-GAVTA was created by PCR amplification of TA4 ORF and then cloned into pCS2-GAVPO cut with *Eco*RI and *Stu*I to remove the p65 domain. Capped messenger RNA was synthesized using the mMESSAGE mMACHINE SP6 kit (Ambion) with pCS2 constructs cut with *Not*I as linear template.

Transgene plasmid mTol2-cryaa:Venus;5xC120:mCherry was created by separate PCR amplification of the *cryaa* promoter plus *venus* ORF (Kurita et al., 2003) and the *5xC120* promoter plus *mcherry* ORF which were then cloned into pminiTol2 (Kawakami et al., 2004; Clark et al., 2011). Transgene plasmid mTol2-cryaa:Venus;5xC120:sox32-P2A-tBFP was created by separate PCR amplification of the *sox32* ORF and the *tagBFP* ORF which were then cloned into mTol2-cryaa:Venus;5xC120:mcherry cut with *Nco*I and *Eco*RV to remove the *mcherry* ORF. The transgene mTol2-cryaa:Venus;5xC120:lefty1 was created by PCR amplification of the *lefty1* ORF from zebrafish cDNA which was then cloned into mTol2-cryaa:Venus;5xC120:mcherry cut with *Nco*I and *Eco*RV to remove the *mcherry* ORF. The transgene pTol2-myl7:GFP;5xC120:Cas9;U6:tyr was created using pDEST-Tol2CG2-U6:gRNA (Ablain et al., 2015) and components from the Gateway Tol2Kit (Kwan et al., 2007). First, a pentameric array of the *C120* promoter was PCR amplified and BP recombination with pDONR-P4-P1R generated the entry vector p5E-5xC120. LR recombination among p5E-5xC120, pME-Cas9 (Leonard Zon, Boston Children's Hospital), p3E-polyA, and pDEST-Tol2CG2-U6:gRNA generated the construct pTol2CG2-U6:gRNA-5xC120:Cas9. This construct was then linearized with *Bse*RI and ligated to an oligonucleotide corresponding to the guide RNA sequence targeting *tyr* (Jao et al., 2013), generating the final transgene plasmid. For the experiments shown in Fig. 5, wild-type embryos were injected at the one-cell stage with 15 pg plasmid, 50 pg transposase mRNA and 50 pg TAEL mRNA. Transgenesis efficiency was assessed by *myl7:GFP* expression.

Zebrafish strains

Adult *Danio rerio* zebrafish were maintained under standard laboratory conditions. Zebrafish with the AB and/or TL background were used as wild-type strains. *Tg(UAS:kaede)*^{rk8Tg} was provided by Herwig Baier (Max Planck Institute of Neurobiology). *Tg(sox17:GFP)*^{s870} (Mizoguchi et al., 2008) and *Tg(myl7:GFP)*^{twu26} (Huang et al., 2003) have been previously described. Transgenes for creating *Tg(cryaa:Venus;C120:mcherry)*^{sfc14} and *Tg(cryaa:Venus;C120:sox32-P2A-tBFP)*^{sfc15} were created as described above. Stable lines were generated using standard transgenesis protocols (Kawakami et al., 2004; Clark et al., 2011). This study was performed in accordance with the Guidelines for Animal Experimentation of National Institutes of Natural Sciences, with approval of the Institutional Animal Care and Use Committee (IACUC) of the National Institutes of Natural Sciences.

Development (2017) 144, 345-355 doi:10.1242/dev.139238

Toxicity curves in zebrafish

To assess the toxicity of the transcriptional activators, 50, 100, 150 or 200 pg of VP-EL222, GAVPO, TA4-EL222, GAVPO(TA4) or GFP (control) mRNA per embryo were injected at the one- to two-cell stage. Unfertilized embryos were removed at 6-8 hpf, and then illuminated globally with blue light. At 1 dpf, injected embryos were scored as unaffected or affected (developmentally deformed or dead) alongside uninjected control embryos from the same clutch. Uninjected control embryos exposed to blue light showed the same levels of toxicity as uninjected control embryos not exposed to blue light. Each group comprised n>100 embryos. Total number of injected and examined embryos is as follows: GAVPO (n=849), EL222 (n=1421), GFP (n=1190), GAVTA (n=809) and TAEL (n=824). Statistical differences in toxicity between transcriptional activators in comparison to GFP control were calculated with Graphpad using Fisher's exact test.

Microscopy and image processing of zebrafish embryos

Fluorescence and bright-field images in Fig. 1 were taken at 24 hpf on a Zeiss Axio Observer.Z1 running Zen Blue, equipped with a X-Cite 120Q fluorescence lamp (Lumen Dynamics), Coolsnap ES2 CCD camera and a 5×0.25NA Fluar Zeiss objective. Dechorionated embryos were embedded in 1.5% low-melt agarose (ISC BioExpress) within glass-bottom Petri dishes (MatTek Corporation). Standard filter settings were applied and bright-field and fluorescence images were then merged. Fluorescence and bright-field images in Fig. 4 were acquired on a Leica dissecting microscope. Fluorescence and bright-field images in Fig. 5 were acquired on a Nikon Eclipse Ti microscope with a 10× objective lens. Identical exposure settings for fluorescence images were used for all embryos from the same set of experiments. All image processing and analysis was performed using ImageJ software (Schneider et al., 2012).

Global light induction

For global light induction, a TaoTronics TT-AL09 120W Dimmable LED Aquarium Hood was used to apply constant or pulsed light (GraLab Model 451 High-Accuracy Digital Electronic Timer). Actual power of light received by embryos (lids of plates removed) was measured as ∼1.6 mW/cm^2 at 456 nm using a PM100D Laser Power and Energy Meter Console (Thorlabs). Dark controls were placed in a lightproof box in the same 30°C incubator as light-treated samples.

Spatial activation

For experiments presented in Fig. 2, *Tg(cryaa:Venus;C120:mcherry)* embryos were injected with 100 pg TAEL mRNA. For embryos activated with the point scanning confocal, embryos were also injected with 100 ng Alexa Fluor 680 dextran (10,000 MW; Life Technologies). At the 10 somite stage, the eye region on one side was illuminated with a 2 min pulse of blue light using one of the four methods described below. After activation, PTU was added to final concentration of 0.003% and embryos were returned to the incubator (in the dark) for another 4-6 h before imaging for mCherry reporter. Analysis of mCherry expression was performed on the Zeiss Axio Observer (see above), except for the experiments involving light patterning with the Leica point scanning confocal, for which we imaged on the same confocal microscope.

Epifluorescence microscopy

A Nikon Eclipse Ti microscope running NIS Elements, equipped with a Sutter Lambda XL Broad Spectrum Light Source, an electron multiplying charge-coupled device (EM-CCD) camera (Andor iXon DU-897) and a 20× Plan Apo 0.75NA Nikon objective was used for epifluorescence microscopy. A 760LP filter was placed in the bright-field path to prevent unwanted activation from bright-field illumination. Standard filter settings were applied and then bright-field and fluorescence images merged. For experiments presented in Fig. 3, *Tg(cryaa:Venus;C120:mcherry); Tg(sox17:GFP)* embryos were injected with 100 pg TAEL mRNA and 100 pg H2B-mCherry mRNA. At 3-4 hpf, embryos were mounted in 1% low-melting agarose within glass-bottom Petri dishes (Mat-Tek) and the animal pole was illuminated with a 2 min pulse of blue light as described above (activation zone in Fig. 3B is ∼116 µm in diameter or 10,568 µm^2). Assessment of *Tg(sox17:GFP)* expression was performed at 6-7 hpf on a Nikon Ti-E microscope equipped with a Yokogawa CSU-22 spinning disk confocal unit. *Z*-stacks at 0.9 µm intervals were acquired with a 20×/0.75NA objective. Maximum *z*-projections and stack re-slicing were performed using ImageJ software. Irradiance was measured to be ∼1800 mW/cm^2 at 488 nm.

Point scanning spectral confocal microscopy

A Leica TCS SPE system running Leica Application Suite, equipped with a 20× HCX Apo 0.5NA water-dipping Leica objective was used for point scanning confocal microscopy. For activation, a single focal plane was continually scanned with the 488 nm laser at 16.6 µW power, 400 Hz speed over a ∼175×175 µm ROI for 2 min. Subsequently, mCherry fluorescence was imaged using the 561 nm laser with emission filter set to 570-650 nm. Alexa Fluor 680 dextran was used for whole-embryo counter-labeling and imaged with the 647 nm laser with emission filter set to 680-800 nm.

DSLM

Embryos were mounted in a 1.5% low-melt agarose cylinder using 3 mm O.D. 2 mm I.D. FEP tubing (Bola). A 10×0.5NA Zeiss objective was used to image the 488 nm activating beam (488 nm laser line and a 488LP filter) and bright-field image (760 nm LED, no filter). The 488 nm laser was continually scanned for 2 min at ∼100 µW power over a range of 133 µm for the 'large beam' and 20 µm for the 'small beam'.

DMD

A Nikon Eclipse Ti microscope running Nikon Elements, equipped with a custom digital micro mirror device (Andor Technologies), an EM-CCD camera (Evolve, Photometrics) and a Nikon 10× Plan Fluor 0.3NA DIC objective was used for DMD. 'On' pixels (regions to be stimulated with activating light) were illuminated with 470 nm light (Lumileds), whereas 'off' pixels were unexposed. Irradiance was measured to be approximately 1.7 mW/cm^2 at 470 nm.

Real-time quantitative PCR

To examine the kinetics of TAEL-induced transcription, *Tg(cryaa:Venus; C120:mcherry)* embryos were injected with 100 pg TAEL mRNA at the one-cell stage. At 3-3.5 hpf (just after the mid-blastula transition), embryos were globally illuminated with 465 nm light; for negative controls, injected embryos were kept in the dark by covering dishes with aluminum foil. At the indicated time points, total RNA was extracted using the RNEasy Kit (Qiagen). 500 ng RNA was used for reverse transcription using the Quantitect cDNA synthesis kit (Qiagen). The qPCR reaction mixture contained 2× SYBR green PCR master mix (Qiagen), 10-fold diluted cDNA and 714 nM each primer. Reactions were carried out in an Applied Biosystems 7900HT Fast Real-Time PCR System (Applied Biosystems) as follows: initial activation at 95°C for 10 min, followed by 40 cycles of 30 s at 95°C, 1 min at 60°C and 1 min at 72°C. Once the PCR was completed, a melt curve analysis was performed to determine reaction specificity. Data in Fig. 1H and Fig. S3 represent averages from three biological replicates each with three technical replicates. The housekeeping gene *ef1a* was used as a reference. Fold change was calculated using the Livak method ($2^{-\Delta\Delta Ct}$) (Livak and Schmittgen, 2001). Statistical significance was determined using Prism software (GraphPad).

qPCR primers used are: *mcherry* forward: 5′-GACCACCTACAAGGC-CAAGA-3′; *mcherry* reverse: 5′-CTCGTTGTGGGAGGTGATGT-3′; *ef1a* forward: 5′-CAAGAAGAGTAGTACCGCTAGCAT-3′; *ef1a* reverse: 5′-CACGGTGACAACATGCTGGAG-3′.

CEL I nuclease assay

Genomic DNA was isolated by placing 2 dpf embryos in lysis solution (10 mM Tris-HCl, pH 8.0, 2 mM EDTA, 0.2% Triton X-100, 1 µg proteinase K) and incubation at 55°C for 2 h followed by heat inactivation of the proteinase K (10 min at 98°C). The region flanking the CRISPR target site of *tyrosinase* was amplified from genomic DNA by PCR. 2 µl 10 mM $MgCl_2$ was then added to 20 µl of each sample. Heteroduplex DNA was

Development (2017) 144, 345-355 doi:10.1242/dev.139238

formed by the following annealing protocol: 98°C for 10 min (initial denaturation) followed by cooling to 25°C at −0.3°C/s. Each sample was then digested with 2 µl CEL I nuclease (gift from Dan Hart, UCSF) at 42°C for 1 h. Samples were resolved by gel electrophoresis in 2% agarose gels stained with ethidium bromide. *tyrosinase* target sequence: 5′-CCCCAGAAGTCCTCCAGTCC-3′; *tyrosinase* forward PCR primer: 5′-GCGTCTCACTCTCCTCGACT-3′; *tyrosinase* reverse PCR primer: 5′-CGCACTGGCAGGTTTGGTTG-3′.

Acknowledgements

We thank the Weiner lab, Hilary Clay, Roland Wu, Stefan Materna and Ian Foe for help throughout this work and critical comments on the manuscript. We thank Daniel Hart for providing CEL I nuclease. We would also like to acknowledge the Cardiovascular Research Institute's Imaging Core and Shaun Coughlin for generously allowing us use of their microscopes. We thank Gary Moulder for excellent fish care.

Competing interests

L.B.M.-M. and K.H.G. are cofounders of Optologix, Inc., which is developing light-regulated transcription factors for research applications.

Author contributions

Conceptualization, A.R., O.D.W., D.Y.S., S.W.; Methodology, A.R., S.W.; Validation, A.R., S.W.; Investigation, A.R., S.W.; Resources, L.B.M.-M., K.H.G.; Writing - original draft, A.R., O.D.W., S.W.; Writing - review and editing, A.R., O.D.W., S.W., D.Y.S., L.B.M.-M., K.H.G.; Supervision, O.D.W., S.W.; Funding acquisition, O.D.W., S.W.

Funding

This work was funded by the National Institutes of Health (NIH) (GM118167) and an American Heart Association established investigator award to O.D.W.; NIH (GM106239) and Cancer Prevention and Research Institute of Texas (RP130312) to K.H.G.; NIH (HL54737) and David and Lucile Packard Foundation funding to D.Y.S.; NIH (DK106358 and DK092312) to S.W. A.R. was supported by a National Science Foundation Graduate Research Fellowship. Deposited in PMC for release after 12 months.

Supplementary information

Supplementary information available online at
http://dev.biologists.org/lookup/doi/10.1242/dev.139238.supplemental

References

Ablain, J., Durand, E. M., Yang, S., Zhou, Y. and Zon, L. I. (2015). A CRISPR/Cas9 vector system for tissue-specific gene disruption in zebrafish. *Dev. Cell* **32**, 756-764.

Alexander, J., Rothenberg, M., Henry, G. L. and Stainier, D. Y. R. (1999). *casanova* plays an early and essential role in endoderm formation in zebrafish. *Dev. Biol.* **215**, 343-357.

Baron, U., Gossen, M. and Bujard, H. (1997). Tetracycline-controlled transcription in eukaryotes: novel transactivators with graded transactivation potential. *Nucleic Acids Res.* **25**, 2723-2729.

Buckley, C. E., Moore, R. E., Reade, A., Goldberg, A. R., Weiner, O. D. and Clarke, J. D. W. (2016). Reversible optogenetic control of subcellular protein localization in a live vertebrate embryo. *Dev. Cell* **36**, 117-126.

Chen, X., Wang, X., Du, Z., Ma, Z. and Yang, Y. (2013). Spatiotemporal control of gene expression in mammalian cells and in mice using the LightOn system. *Curr. Protoc. Chem. Biol.* **5**, 111-129.

Clark, K. J., Urban, M. D., Skuster, K. J. and Ekker, S. C. (2011). Transgenic zebrafish using transposable elements. *Methods Cell Biol.* **104**, 137-149.

Crosson, S., Rajagopal, S. and Moffat, K. (2003). The LOV domain family: photoresponsive signaling modules coupled to diverse output domains. *Biochemistry* **42**, 2-10.

Distel, M., Wullimann, M. F. and Köster, R. W. (2009). Optimized Gal4 genetics for permanent gene expression mapping in zebrafish. *Proc. Natl. Acad. Sci. USA* **106**, 13365-13370.

Essner, J. J., Branford, W. W., Zhang, J. and Yost, H. J. (2000). Mesendoderm and left-right brain, heart and gut development are differentially regulated by pitx2 isoforms. *Development* **127**, 1081-1093.

Feldman, B., Gates, M. A., Egan, E. S., Dougan, S. T., Rennebeck, G., Sirotkin, H. I., Schier, A. F. and Talbot, W. S. (1998). Zebrafish organizer development and germ-layer formation require nodal-related signals. *Nature* **395**, 181-185.

Gibson, D. G., Young, L., Chuang, R.-Y., Venter, J. C., Hutchison, C. A. and Smith, H. O. (2009). Enzymatic assembly of DNA molecules up to several hundred kilobases. *Nat. Methods* **6**, 343-345.

Gritsman, K., Zhang, J., Cheng, S., Heckscher, E., Talbot, W. S. and Schier, A. F. (1999). The EGF-CFC protein one-eyed pinhead is essential for nodal signaling. *Cell* **97**, 121-132.

Haffter, P., Odenthal, J., Mullins, M. C., Lin, S., Farrell, M. J., Vogelsang, E., Haas, F., Brand, M., van Eeden, F. J. M., Furutani-Seiki, M. et al. (1996). Mutations affecting pigmentation and shape of the adult zebrafish. *Dev. Genes Evol.* **206**, 260-276.

Halpern, M. E., Rhee, J., Goll, M. G., Akitake, C. M., Parsons, M. and Leach, S. D. (2008). Gal4/UAS transgenic tools and their application to zebrafish. *Zebrafish* **5**, 97-110.

Hesselson, D., Anderson, R. M., Beinat, M. and Stainier, D. Y. R. (2009). Distinct populations of quiescent and proliferative pancreatic beta-cells identified by HOTcre mediated labeling. *Proc. Natl. Acad. Sci. USA* **106**, 14896-14901.

Huang, C.-J., Tu, C.-T., Hsiao, C.-D., Hsieh, F.-J. and Tsai, H.-J. (2003). Germ-line transmission of a myocardium-specific GFP transgene reveals critical regulatory elements in the cardiac myosin light chain 2 promoter of zebrafish. *Dev. Dyn.* **228**, 30-40.

Jao, L.-E., Wente, S. R. and Chen, W. (2013). Efficient multiplex biallelic zebrafish genome editing using a CRISPR nuclease system. *Proc. Natl. Acad. Sci. USA* **110**, 13904-13909.

Kawakami, K., Takeda, H., Kawakami, N., Kobayashi, M., Matsuda, N. and Mishina, M. (2004). A transposon-mediated gene trap approach identifies developmentally regulated genes in zebrafish. *Dev. Cell* **7**, 133-144.

Kennedy, M. J., Hughes, R. M., Peteya, L. A., Schwartz, J. W., Ehlers, M. D. and Tucker, C. L. (2010). Rapid blue-light-mediated induction of protein interactions in living cells. *Nat. Methods* **7**, 973-975.

Kikuchi, Y., Agathon, A., Alexander, J., Thisse, C., Waldron, S., Yelon, D., Thisse, B. and Stainier, D. Y. (2001). casanova encodes a novel Sox-related protein necessary and sufficient for early endoderm formation in zebrafish. *Genes Dev.* **15**, 1493-1505.

Kimmel, C. B., Warga, R. M. and Schilling, T. F. (1990). Origin and organization of the zebrafish fate map. *Development* **108**, 581-594.

Knopf, F., Schnabel, K., Haase, C., Pfeifer, K., Anastassiadis, K. and Weidinger, G. (2010). Dually inducible TetON systems for tissue-specific conditional gene expression in zebrafish. *Proc. Natl. Acad. Sci. USA* **107**, 19933-19938.

Kurita, R., Sagara, H., Aoki, Y., Link, B. A., Arai, K.-I. and Watanabe, S. (2003). Suppression of lens growth by alphaA-crystallin promoter-driven expression of diphtheria toxin results in disruption of retinal cell organization in zebrafish. *Dev. Biol.* **255**, 113-127.

Kwan, K. M., Fujimoto, E., Grabher, C., Mangum, B. D., Hardy, M. E., Campbell, D. S., Parant, J. M., Yost, H. J., Kanki, J. P. and Chien, C.-B. (2007). The Tol2kit: a multisite gateway-based construction kit for Tol2 transposon transgenesis constructs. *Dev. Dyn.* **236**, 3088-3099.

Liu, H., Gomez, G., Lin, S., Lin, S. and Lin, C. (2012). Optogenetic control of transcription in zebrafish. *PLoS ONE* **7**, e50738.

Livak, K. J. and Schmittgen, T. D. (2001). Analysis of relative gene expression data using real-time quantitative PCR and the $2^{-\Delta\Delta CT}$ method. *Methods* **25**, 402-408.

Maizel, A., von Wangenheim, D., Federici, F., Haseloff, J. and Stelzer, E. H. K. (2011). High-resolution live imaging of plant growth in near physiological bright conditions using light sheet fluorescence microscopy. *Plant J.* **68**, 377-385.

Mizoguchi, T., Verkade, H., Heath, J. K., Kuroiwa, A. and Kikuchi, Y. (2008). Sdf1/Cxcr4 signaling controls the dorsal migration of endodermal cells during zebrafish gastrulation. *Development* **135**, 2521-2529.

Motta-Mena, L. B., Reade, A., Mallory, M. J., Glantz, S., Weiner, O. D., Lynch, K. W. and Gardner, K. H. (2014). An optogenetic gene expression system with rapid activation and deactivation kinetics. *Nat. Chem. Biol.* **10**, 196-202.

Nash, A. I., McNulty, R., Shillito, M. E., Swartz, T. E., Bogomolni, R. A., Luecke, H. and Gardner, K. H. (2011). Structural basis of photosensitivity in a bacterial light-oxygen-voltage/helix-turn-helix (LOV-HTH) DNA-binding protein. *Proc. Natl. Acad. Sci. USA* **108**, 9449-9454.

Nihongaki, Y., Kawano, F., Nakajima, T. and Sato, M. (2015). Photoactivatable CRISPR-Cas9 for optogenetic genome editing. *Nat. Biotechnol.* **33**, 755-760.

Ohlendorf, R., Vidavski, R. R., Eldar, A., Moffat, K. and Möglich, A. (2012). From dusk till dawn: one-plasmid systems for light-regulated gene expression. *J. Mol. Biol.* **416**, 534-542.

Peyriéras, N., Strähle, U. and Rosa, F. (1998). Conversion of zebrafish blastomeres to an endodermal fate by TGF-beta-related signaling. *Curr. Biol.* **8**, 783-788.

Pézeron, G., Mourrain, P., Courty, S., Ghislain, J., Becker, T. S., Rosa, F. M. and David, N. B. (2008). Live analysis of endodermal layer formation identifies random walk as a novel gastrulation movement. *Curr. Biol.* **18**, 276-281.

Polstein, L. R. and Gersbach, C. A. (2012). Light-inducible spatiotemporal control of gene activation by customizable zinc finger transcription factors. *J. Am. Chem. Soc.* **134**, 16480-16483.

Polstein, L. R. and Gersbach, C. A. (2015). A light-inducible CRISPR-Cas9 system for control of endogenous gene activation. *Nat. Chem. Biol.* **11**, 198-200.

Development (2017) 144, 345-355 doi:10.1242/dev.139238

Rebagliati, M. R., Toyama, R., Fricke, C., Haffter, P. and Dawid, I. B. (1998). Zebrafish nodal-related genes are implicated in axial patterning and establishing left-right asymmetry. *Dev. Biol.* **199**, 261-272.

Rivera-Cancel, G., Motta-Mena, L. B. and Gardner, K. H. (2012). Identification of natural and artificial DNA substrates for light-activated LOV-HTH transcription factor EL222. *Biochemistry* **51**, 10024-10034.

Sakai, S., Ueno, K., Ishizuka, T. and Yawo, H. (2013). Parallel and patterned optogenetic manipulation of neurons in the brain slice using a DMD-based projector. *Neurosci. Res.* **75**, 59-64.

Sander, J. D. and Joung, J. K. (2014). CRISPR-Cas systems for editing, regulating and targeting genomes. *Nat. Biotechnol.* **32**, 347-355.

Schneider, C. A., Rasband, W. S. and Eliceiri, K. W. (2012). NIH Image to ImageJ: 25 years of image analysis. *Nat. Methods* **9**, 671-675.

Scott, E. K. and Baier, H. (2009). The cellular architecture of the larval zebrafish tectum, as revealed by Gal4 enhancer trap lines. *Frontiers Neural Circuits* **3**, 13.

Shimizu-Sato, S., Huq, E., Tepperman, J. M. and Quail, P. H. (2002). A light-switchable gene promoter system. *Nat. Biotechnol.* **20**, 1041-1044.

Shoji, W. and Sato-Maeda, M. (2008). Application of heat shock promoter in transgenic zebrafish. *Dev. Growth Differ.* **50**, 401-406.

Thisse, C. and Thisse, B. (1999). Antivin, a novel and divergent member of the TGFbeta superfamily, negatively regulates mesoderm induction. *Development* **126**, 229-240.

Thisse, B., Wright, C. V. E. and Thisse, C. (2000). Activin- and Nodal-related factors control antero-posterior patterning of the zebrafish embryo. *Nature* **403**, 425-428.

Till, B. J., Burtner, C., Comai, L. and Henikoff, S. (2004). Mismatch cleavage by single-strand specific nucleases. *Nucleic Acids Res.* **32**, 2632-2641.

Tischer, D. and Weiner, O. D. (2014). Illuminating cell signalling with optogenetic tools. *Nat. Rev. Mol. Cell Biol.* **15**, 551-558.

Wang, X., Chen, X. and Yang, Y. (2012). Spatiotemporal control of gene expression by a light-switchable transgene system. *Nat. Methods* **9**, 266-269.

Yan, Y.-T., Gritsman, K., Ding, J., Burdine, R. D., Corrales, J. D., Price, S. M., Talbot, W. S., Schier, A. F. and Shen, M. M. (1999). Conserved requirement for EGF-CFC genes in vertebrate left-right axis formation. *Genes Dev.* **13**, 2527-2537.

Yazawa, M., Sadaghiani, A. M., Hsueh, B. and Dolmetsch, R. E. (2009). Induction of protein-protein interactions in live cells using light. *Nat. Biotechnol.* **27**, 941-945.

Ye, H., Baba, M. D.-E., Peng, R.-W. and Fussenegger, M. (2011). A synthetic optogenetic transcription device enhances blood-glucose homeostasis in mice. *Science* **332**, 1565-1568.

Zoltowski, B. D., Motta-Mena, L. B. and Gardner, K. H. (2013). Blue light-induced dimerization of a bacterial LOV-HTH DNA-binding protein. *Biochemistry* **52**, 6653-6661.

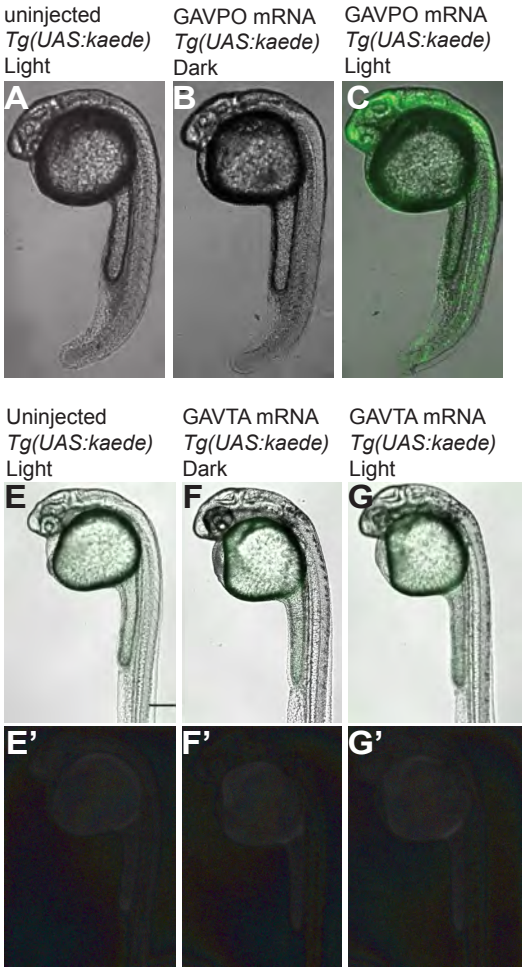

Figure S1: LightOn system induces kaede expres-sion from the UAS promoter in a light-gated manner. A-C. Tg(UAS:kaede) embryos were injected with GAVPO mRNA and then illuminated with con-stant, global blue light (465 nm) from approximately 4-24 hpf (hours post-fertilization). GAVPO injected embryos showed robust induction of Kaede fluores-cent protein at 24 hpf (C), with no visible induction of Kaede expression in dark (B) or uninjected controls (A). **D-F**. Following blue light illumination, GAVTA is unable to induce transcription of kaede from the UAS promoter (F, F').

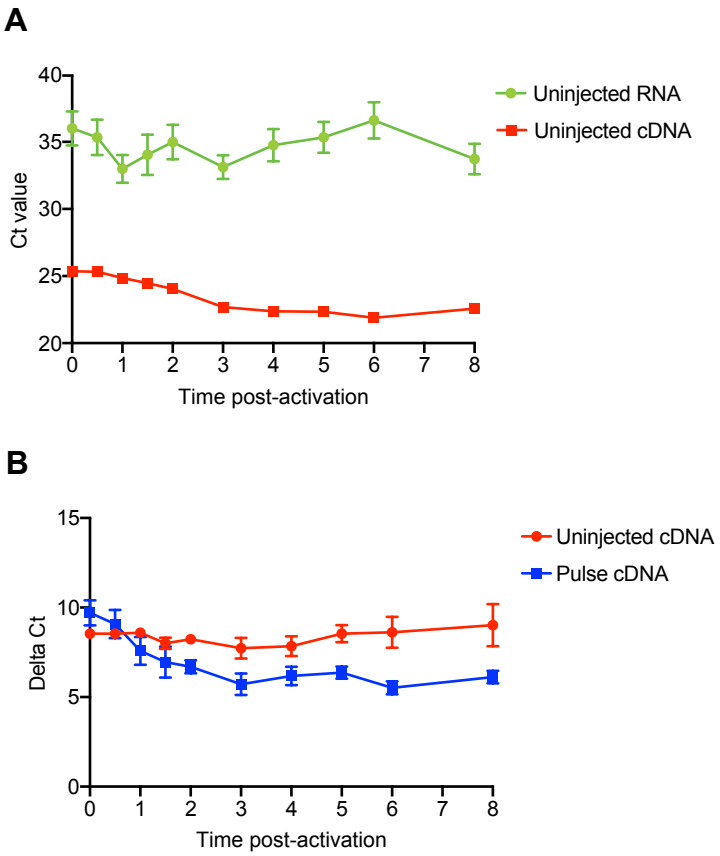

Figure S2. Assessing leakiness of the C120 promoter.
Uninjected *Tg(cryaa:Venus;C120:mcherry)* embryos were globally illuminated with pulsed 465 nm light (1 hour on, 1 hour off) starting at 3-3.5 hpf and mCherry mRNA levels were measured at the indicated time points by qPCR. **A**. Average uncorrected CT values suggest that low-level mCherry expression can be detected in uninjected embryos (red line). This signal is likely not due to contaminating genomic DNA as qPCR using total RNA rather than cDNA as template resulted in CT values > 10 cycles higher. **B**. Delta-CT measurements show that relative mCherry expression remains low and unchanged in uninjected embryos (red line) compared to embryos injected with 100 pg TAEL mRNA and illuminated with pulsed blue light (blue line). Delta-Ct = CT(mCherry)-CT(ef1a).

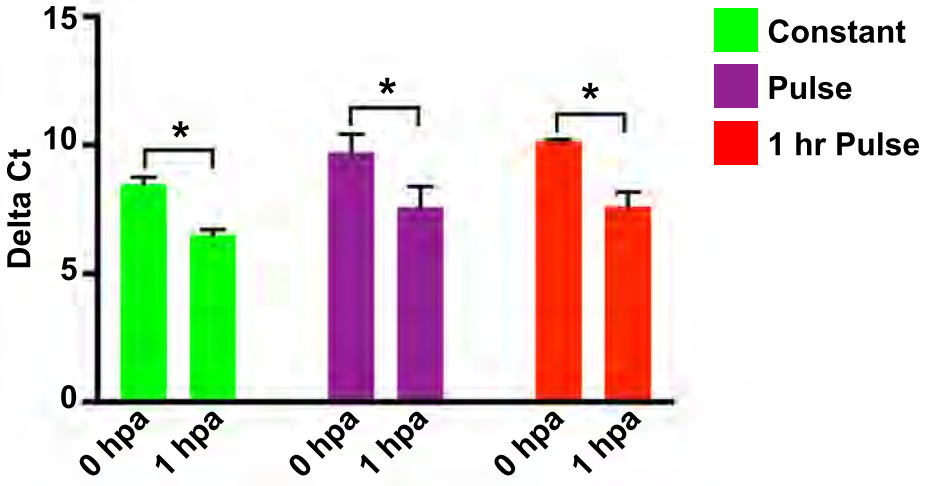

Figure S3. mCherry expression is significantly upregulated at 1 hour post-activation. Tg(cryaa:Venus; 5xC120:mCherry) embryos were injected with 100 pg TAEL mRNA and globally illuminated with 465 nm light. Levels of mCherry expression were measured by qPCR. Delta-Ct measurements show that mCherry expression is significantly upregulated at 1 hour post-activation for all illumination patterns tested. Delta Ct = Ct(mCherry) – Ct(ef1a). hpa, hours post-activation. *p<0.05 by paired t-test. Error bars, S.E.M.

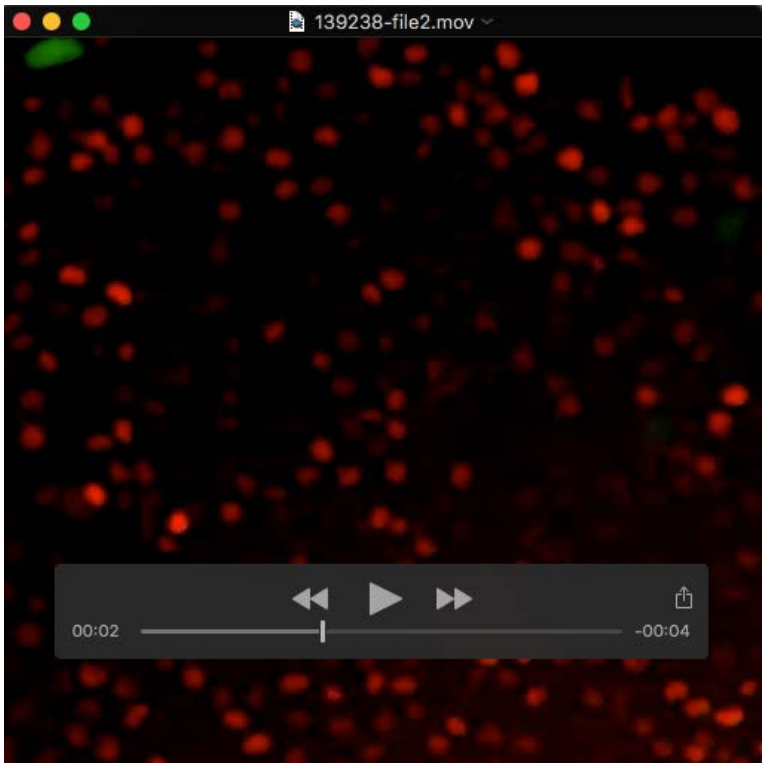

Movie 1: Canonical endoderm (*sox17)* expression profile.

Z-stack through a *Tg(cryaa:Venus; 5xC120:sox32); Tg(sox17:GFP)* embryo at approximately 70% epiboly. The embryo was injected with H2B-mCherry mRNA to label all nuclei (red). Images were acquired every 0.9 µm on a Nikon Ti-E microscope equipped with a Yokogawa CSU-22 spinning disk confocal unit. The z-stack starts at the embryo surface and goes through towards the yolk. *Tg(sox17:GFP)* expression (green) appears in only at the innermost layer closest to at the yolk, consistent with endogenous endoderm localization.

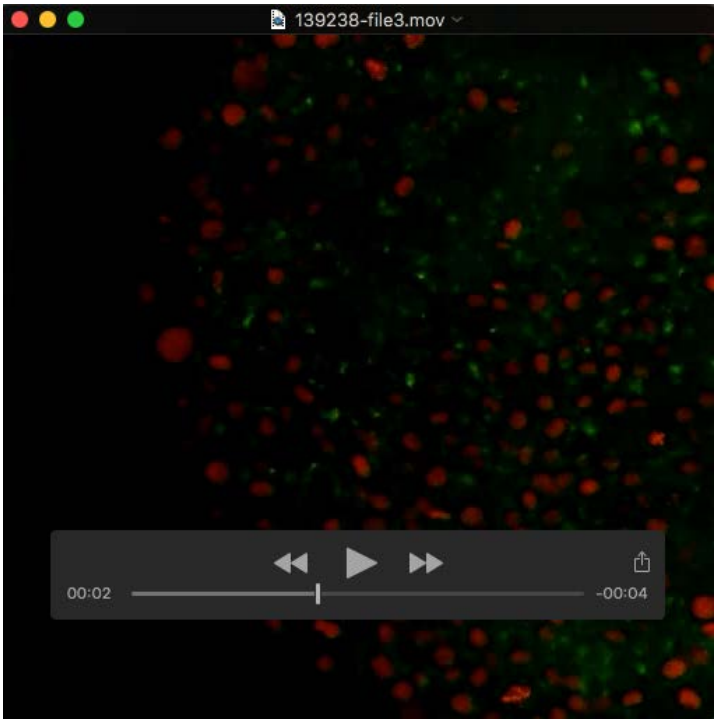

Movie 2: Ectopic endoderm is not induced when TAEL injected embryos are kept in the dark.

Z-stack through a *Tg(cryaa:Venus; 5xC120:sox32); Tg(sox17:GFP)* embryo at approximately 70% epiboly. The embryo was injected with H2B-mCherry mRNA to label all nuclei (red) and TAEL mRNA, then kept in the dark until image acquisition. Images were acquired every 0.9 µm on a Nikon Ti-E microscope equipped with a Yokogawa CSU-22 spinning disk confocal unit. The z-stack starts at the embryo surface and goes through towards the yolk. *Tg(sox17:GFP)* expression (green) appears in only at the innermost layer closest to at the yolk, consistent with endogenous endoderm localization.

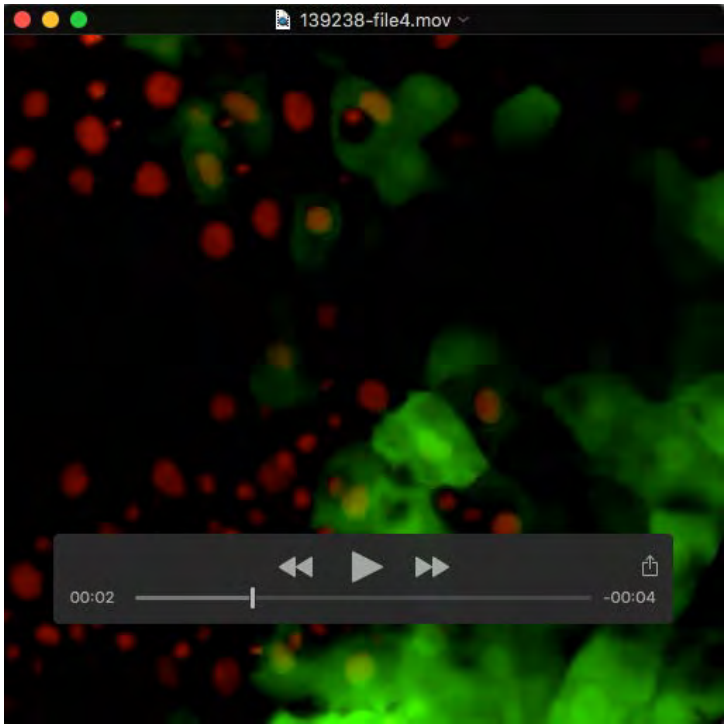

Movie 3: Ectopic endoderm induction via over-expression of Sox32.
Z-stack through a *Tg(cryaa:Venus; 5xC120:sox32); Tg(sox17:GFP)* embryo at approximately 70% epiboly. The embryo was injected with H2B-mCherry mRNA to label all nuclei (red) and TAEL mRNA. At 3-4 hpf, the animal pole was illuminated with a 2 min pulse of blue light to activate TAEL-dependent *sox32* expression. Images were acquired every 0.9 µm on a Nikon Ti-E microscope equipped with a Yokogawa CSU-22 spinning disk confocal unit. The z-stack starts at the embryo surface and goes through towards the yolk. *Tg(sox17:GFP)* expression (green) is apparent in the outermost cell layers as well as within the endogenous endoderm layer.